Received 20 June 2023; revised 26 August 2023 and 9 September 2023; accepted 7 October 2023. Date of publication 12 October 2023; date of current version 27 October 2023. The review of this article was arranged by Editor H. Ma.

*Digital Object Identifier 10.1109/JEDS.2023.3324065*

# Analog PWM Method With Sweep Generation Structure Based on P-Type LTPS TFTs for Micro-LED Displays

**CHIH-LUNG LIN [1] (Senior Member, IEEE), CHENG-HAN KE [1] (Student Member, IEEE), JUI-HUNG CHANG [1] (Graduate Student Member, IEEE), CHIEH-AN LIN [2], CHIA-EN WU [3], AND MING-HSIEN LEE [3]**

1 Department of Electrical Engineering, National Cheng Kung University, Tainan City 70101, Taiwan
2 Department of TCON Digital IC, Raydium Semiconductor Corporation, Hsinchu 300, Taiwan
3 Display Technology Research and Development Department IT, AUO Corporation, Hsinchu 300094, Taiwan

CORRESPONDING AUTHOR: C.-L. LIN (e-mail: cllin@ee.ncku.edu.tw)

This work was supported in part by the National Science and Technology Council of Taiwan under Project NSTC 110-2221-E-006-149-MY3, and in part by AUO Corporation.

**ABSTRACT** This work proposes a novel pixel circuit using analog pulse width modulation (PWM) for micro light-emitting diode (micro-LED) displays. The proposed circuit generates uniform sweep waveforms and driving currents to control micro-LED emission precisely by compensating for threshold voltage ($V_{TH}$) variations of p-type low-temperature polycrystalline silicon thin-film transistors (LTPS TFTs) and $V_{DD}$ current-resistance drops (I-R drops). Driven by the PWM method, micro-LED can operate with high wall-plug efficiency (WPE), leading to low power consumption. To analyze the circuit performance, the electrical characteristics of a micro-LED and LTPS TFTs are measured to establish the simulated models. The HSPICE simulation results present that the current error rates and time shift rates of emission currents are below 1.65% and 2.75%, respectively, with ±0.3 V variations in $V_{TH}$ and 1.2 V drops in $V_{DD}$. Furthermore, the power improvement relative to a 7T1C pulse amplitude modulation (PAM) circuit is higher than 19.05% at all gray levels, confirming that the proposed circuit is suitable for use in micro-LED displays.

**INDEX TERMS** Low-temperature polycrystalline silicon thin-film transistor (LTPS TFT), micro light-emitting diode (micro-LED), pulse width modulation (PWM), power consumption.

## I. INTRODUCTION

Over the past decade, many consumer electronics with brilliant panels have been produced and provide excellent visual experiences. In the next generation, micro light-emitting diode (micro-LED) displays are highly attractive owing to their excellent brightness, wide color gamut, and extreme contrast ratio [1]. Micro-LEDs are fabricated from inorganic material, and they do not suffer from burn-in encountered by organic light-emitting diodes (OLEDs) and have a long lifespan [2]. For the thin-film transistor (TFT) backplanes of OLED displays, amorphous indium-gallium-zinc oxide (a-IGZO) and low-temperature polycrystalline silicon (LTPS) technologies are mature and widely used. However, to drive the micro-LED in a high current over the long term, LTPS TFTs, which possess excellent mobility and reliability, are preferred for micro-LED display [3], [4]. Although the threshold voltage ($V_{TH}$) variations of LTPS TFTs influence the emission currents and generate mura defects in the displays [5], many pulse amplitude modulation (PAM) circuits for pixels have been proposed to address the $V_{TH}$ variation issue [6], [7], [8]. Lee et al. presented a 7T1C PAM circuit that can sense and compensate for the $V_{TH}$ of driving TFT (T1) in Fig. 1 [8]. Nevertheless, the 7T1C circuit is unsuitable for micro-LED displays because the emission wavelength of micro-LED varies with current density [9]. Also, the wall-plug efficiency (WPE) of micro-LEDs is poor at low current densities [10]. To achieve the required luminance, larger currents must be provided

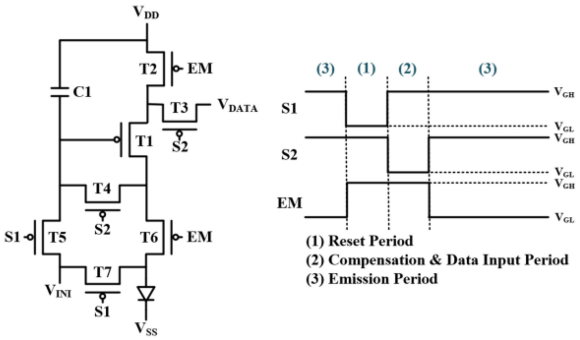


**FIGURE 1.** Schematic and timing diagram of 7T1C PAM circuit [8].

to micro-LEDs, increasing the power consumption of the displays [11]. Therefore, circuits in micro-LED displays have adopted analog pulse width modulation (PWM) to control the emission time with a constant current and determine gray levels [12], [13], [14], [15], [16], [17]. Oh et al. developed a PWM circuit implemented in the micro-LED TV application [14]. The circuit consists of LTPS TFTs, which have the capability of generating the required high current density. Micro-LEDs can thus operate at high luminous efficiency and with low wavelength shifts when emitting light. Zou et al. analyzed the performance of PWM circuits with and without $V_{TH}$ compensation of driving and PWM TFTs [16]. The analysis result presents slight error rates of current amplitude and pulse width after $V_{TH}$ compensation. The uniformity of micro-LED displays is improved. In addition to $V_{TH}$ variations of TFTs, the current-resistance rises and drops (I-R rises/drops) in the power lines will result in varying emission currents [18]. In the previous work, we presented a PWM driving circuit based on n-type LTPS TFTs to eliminate the effect of $V_{SS}$ I-R rises [17]. By the voltage feedback mechanism, the emission currents can be maintained even with different voltage variations. However, to realize PWM, sweep waveforms with different phases are required to control the emission time row by row. The necessary sweep integrated circuit (IC) and sweep gate drivers increase the costs of development and fabrication [19].

Hence, this work proposes a novel analog PWM circuit with a sweep generation structure for micro-LED displays. The circuit compensates for $V_{TH}$ variations of p-type LTPS TFTs and $V_{DD}$ I-R drops and provides stable emission current to micro-LED. According to the required gray levels, different sweep waveforms can be generated to modulate the emission time of micro-LED. Furthermore, to assess the suitability of the proposed circuit for micro-LED displays, a comparison between the proposed and 7T1C circuits is conducted in terms of power consumption.

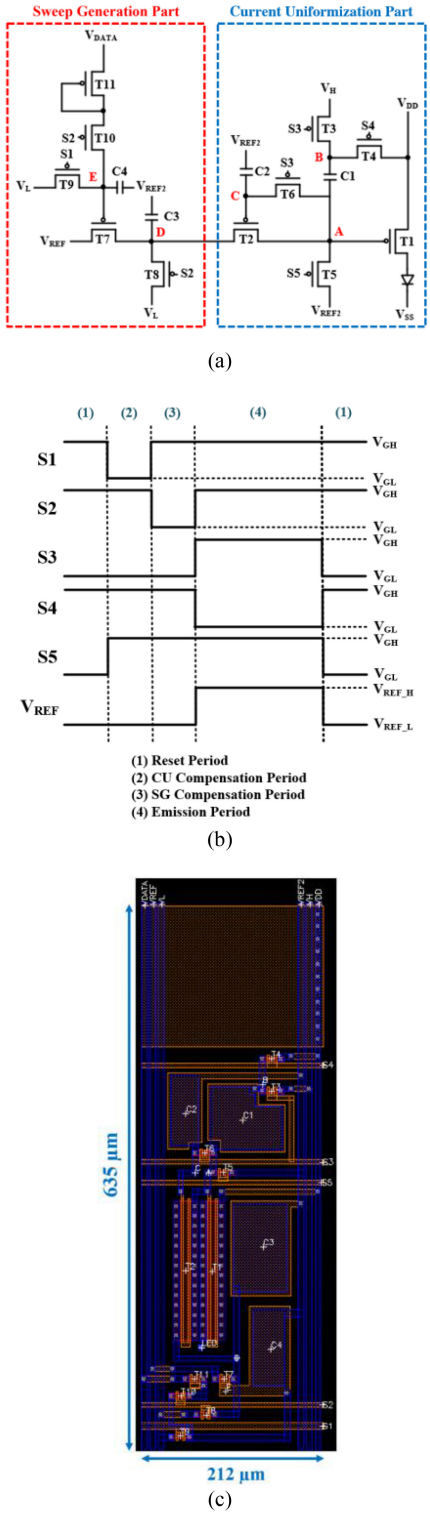


**FIGURE 2.** (a) Schematic, (b) timing diagram, and (c) layout image of proposed pixel circuit.

## II. OPERATION

Figs. 2(a), 2(b), and 2(c) present the schematic, timing diagram, and layout image of the proposed pixel circuit, respectively. The circuit comprises eleven TFTs (T1-T11) and four capacitors (C1-C4), where T1-T6 are for current uniformization (CU), and T7-T11 are for sweep generation (SG) to realize PWM. In the CU part, T1 is a driving TFT to supply a stable current to the micro-LEDs, while T2 is a PWM TFT to control the switching of T1, modulating the pulse width of the emission current. In addition, to compensate for the $V_{TH}$ variations of T1, T1 and T2 are

matched TFTs to have the same aspect ratio and are located adjacently in the layout, exhibiting identical electrical characteristics [20], [21], [22]. In the SG part, T7 provides a sweep-generation current ($I_{SWEEP}$) to charge C3 slowly, and a sweep waveform is generated at node D. Since $V_{TH}$ variations of T7 distort $I_{SWEEP}$, T7 is designed to match T11 for the $V_{TH}$ compensation of T7. The operation in each period is described below in detail.

### A. RESET PERIOD

S3 and S5 are at $V_{GL}$ to turn on T3, T5, and T6, while S1, S2, and S4 are at $V_{GH}$ to turn off T4, T8, T9, and T10. The voltages of nodes A and C ($V_A$ and $V_C$) are reset to $V_{REF2}$, and that of node B ($V_B$) is increased to $V_H$. Since $V_{REF2}$ equals $V_{DD}$, T1 at the cut-off region prevents micro-LED from emitting, suppressing the flicker phenomenon.

### B. CU COMPENSATION PERIOD

S1 goes to $V_{GL}$ to turn on T9, and S5 goes to $V_{GH}$ to turn off T5. The voltage of node E ($V_E$) is decreased to $V_L$, causing T7 to be in the on-state. Hence, $V_{REF\_L}$ starts to charge nodes A and C. Because of the diode-connection structure of T2, $V_A$ and $V_C$ can be increased to $V_{REF\_L} - |V_{TH\_T2}|$, where $V_{TH\_T2}$ is the threshold voltage of T2 and equals that of T1 ($V_{TH\_T1}$).

### C. SG COMPENSATION PERIOD

S1 goes $V_{GH}$ to turn off T9, and S2 goes $V_{GL}$ to turn on T8 and T10. T11 is diode-connected and thus node E is charged to $V_{DATA} - |V_{TH\_T11}|$ to compensate for the $V_{TH}$ of T7, where $V_{TH\_T11}$ is the threshold voltage of T11 and identical to that of T7 ($V_{TH\_T7}$). As the gate voltage of T7 ($V_E$) is increased above its source voltage, T7 is turned off. The voltage of node D ($V_D$) is decreased to $V_L$. Herein, $V_L$ is lower than $V_A$ and $V_C$, so T2 is turned off, enabling $V_A$ and $V_C$ to remain at $V_{REF\_L} - |V_{TH\_T2}|$.

### D. EMISSION PERIOD

S2 and S3 are at $V_{GH}$ to turn off T3, T6, T8, and T10, while S4 is at $V_{GL}$ to turn on T4. $V_B$ is discharged to $V_{DD}$, and $V_A$ changes to $V_{REF\_L} - |V_{TH\_T2}| - V_H + V_{DD}$ due to the capacitive coupling effect of C1. Subsequently, T1 operates at the saturation region and begins to provide an emission current to the micro-LED. The magnitude of the emission current ($I_{LED}$) is derived as follows.

$$\begin{aligned} I_{LED} &= \frac{1}{2}k_{T1}\left(V_{SG\_T1} - |V_{TH\_T1}|\right)^2 \\ &= \frac{1}{2}k_{T1}\left[V_{DD} - \left(V_{REF\_L} - |V_{TH\_T2}| - V_H + V_{DD}\right) \right. \\ &\quad \left. - |V_{TH\_T1}|\right]^2 \\ &= \frac{1}{2}k_{T1}\left(V_H - V_{REF\_L}\right)^2 \end{aligned} \tag{1}$$

where $k_{T1}$ is $\mu \cdot C_{OX} \cdot W/L$ for T1. In Eq. (1), $V_{TH\_T1}$ and $V_{DD}$ are eliminated, eliminating the threshold voltage variations and $V_{DD}$ I-R drops. Meanwhile, $V_{REF}$ is changed from $V_{REF\_L}$ to $V_{REF\_H}$, and $V_E$ remains at $V_{DATA} - |V_{TH\_T11}|$, so T7 is activated and charges node D with $I_{SWEEP}$. The equation for $I_{SWEEP}$ is as follows.

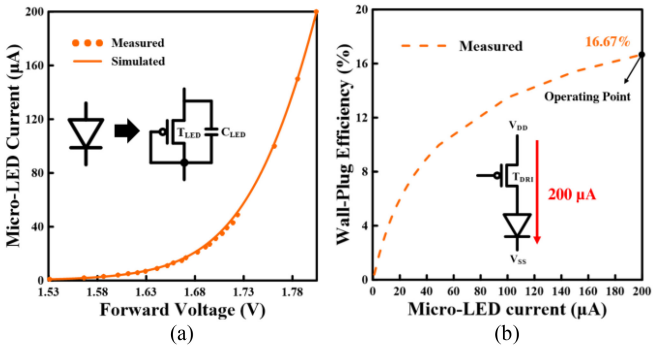


**FIGURE 3.** (a) I-V curve and (b) wall-plug efficiency of fabricated micro-LED.

$$\begin{aligned} I_{SWEEP} &= \frac{1}{2}k_{T7}\left(V_{SG\_T7} - |V_{TH\_T7}|\right)^2 \\ &= \frac{1}{2}k_{T7}\left(V_{REF\_H} - \left(V_{DATA} - |V_{TH\_T11}|\right)\right. \\ &\quad \left. - |V_{TH\_T7}|\right)^2 \\ &= \frac{1}{2}k_{T7}\left(V_{REF\_H} - V_{DATA}\right)^2 \end{aligned} \tag{2}$$

where $k_{T7}$ is $\mu \cdot C_{OX} \cdot W/L$ for T7. In Eq. (2), $I_{SWEEP}$ is unaffected by the $V_{TH\_T7}$ variations and depends only on $V_{DATA}$. Thus, the magnitude of $I_{SWEEP}$ determines the charging rate for node D, and the highly uniform sweep waveforms are generated when the same $V_{DATA}$ is input. Subsequently, $V_D$ will increase and meet the below condition to turn on T2.

$$\begin{aligned} V_{SG\_T2} &= V_D - V_C > |V_{TH\_T2}| \\ &\Rightarrow V_D - \left(V_{REF\_L} - |V_{TH\_T2}|\right) > |V_{TH\_T2}| \\ &\Rightarrow V_D > V_{REF\_L} \end{aligned} \tag{3}$$

According to Eq. (3), the turn-on condition is independent of the variations of $V_{TH\_T2}$. When T2 is on-state, node A is charged to $V_{REF\_H}$, which is higher than the source voltage of T1. T1 is in the cut-off region and ceases to provide the emission current to the micro-LED.

Owing to its sequence of operations, the circuit can alleviate the effects of the $V_{TH\_T1}$ variations and $V_{DD}$ I-R drops on the emission current. By utilizing a stable high current, the micro-LED can be effectively driven at high luminous efficiency, reducing the power consumption of the circuit. Additionally, to realize the precise PWM control, uniform sweep waveforms are obtained by compensating for $V_{TH\_T7}$. Also, the turn-on condition of T2 is not influenced by $V_{TH\_T2}$, which ensures that the emission time is independent of $V_{TH\_T2}$.

## III. RESULTS AND DISCUSSION

Fig. 3(a) shows the emission current to the forward voltage curve of the fabricated micro-LED. Forward voltage refers to the positive voltage applied from the anode to the cathode of a micro-LED, enabling it to conduct current and

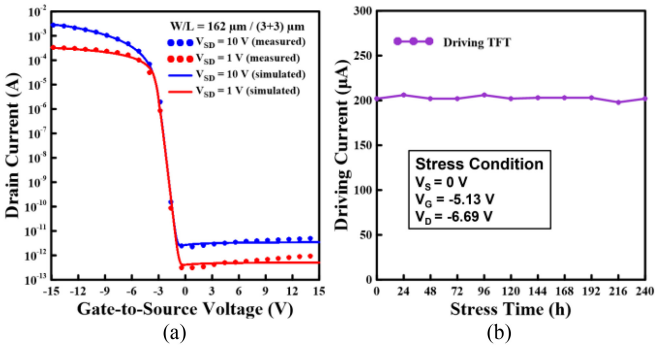


**FIGURE 4.** (a) Transfer characteristics and (b) reliability test under continuous stress of driving TFT.

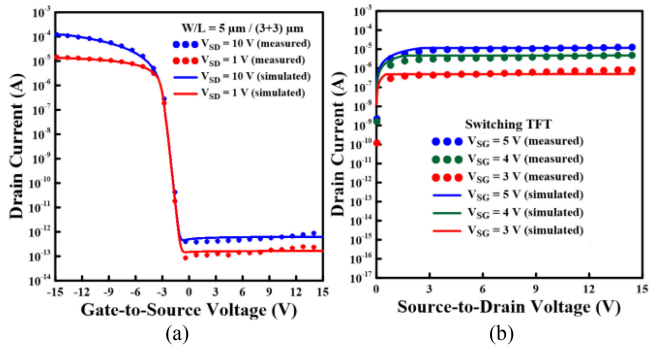


**FIGURE 5.** (a) Transfer and (b) output curves of switching TFT.

**TABLE 1.** Design parameters of proposed pixel circuit.

| Proposed Pixel Circuit | | | |
|---|---|---|---|
| Parameter | Value | Parameter | Value |
| $(W/L)_{T1,\,T2}$ (μm/μm) | 162 / (3+3) | S1-S5 (V) | -5 ~ 13 |
| $(W/L)_{T3\text{-}T11}$ (μm/μm) | 5 / (3+3) | $V_{DATA}$ (V) | 8.89 ~ 11.59 |
| C1, C3 (pF) | 2 | $V_{REF}$ (V) | 7 ~ 12 |
| C2, C4 (pF) | 1 | $V_{REF2}$ (V) | 4 |
| $V_{DD}$ (V) | 4 | $V_H$ (V) | 10.31 |
| $V_{SS}$ (V) | -4.5 | $V_L$ (V) | -2.5 |
| **Equivalent Model of Micro-LED** | | | |
| Parameter | Value | Parameter | Value |
| $(W/L)_{LED}$ (μm/μm) | 162 / (3+3) | $C_{LED}$ (pF) | 0.2 |

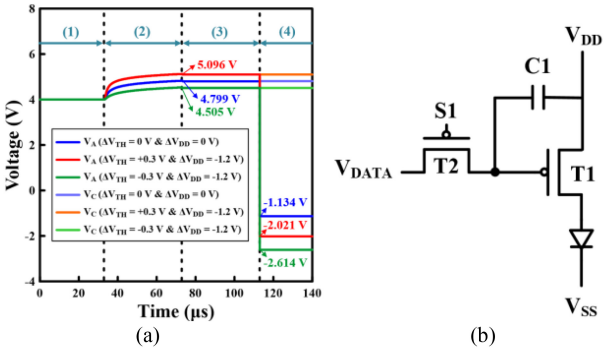


**FIGURE 6.** (a) Transient waveforms of $V_A$ and $V_C$ with $V_{TH}$ variations ($\Delta V_{TH} = \pm$ 0.3 V) of T1 and T2 and $V_{DD}$ I-R drop ($\Delta V_{DD} = -1.2$ V). (b) Schematic of conventional 2T1C circuit.

emit light. The micro-LED with a chip size of 93 $\mu$m $\times$ 150 $\mu$m is designed for RGB displays. An equivalent model of a diode-connected TFT in parallel with a capacitor in an HSPICE simulator represents the behavior of micro-LEDs. The driving current of micro-LED is selected at 200 $\mu$A, corresponding to a high WPE of 16.67% as shown in Fig. 3(b). Fig. 4(a) shows the transfer characteristics of the driving TFT. The driving TFT can provide an emission current of about 200 $\mu$A to micro-LED when operating in the saturation region with $V_{SG}$ and $V_{SD}$ values of 5.13 V and 6.69 V. To verify the reliability of driving TFT, Fig. 4(b) presents its performance under the stress where $V_S$, $V_G$, and $V_D$ are 0 V, $-5.13$ V, and $-6.69$ V, respectively. The driving current remains almost constant during a stress period of 240 h. Figs. 5(a) and 5(b) show the transfer and output curves of the switching TFT. The switching TFT can serve as a switch and as T7 to generate constant currents in the saturation region. Furthermore, Rensselaer Polytechnic Institute (RPI) poly-Si TFT models (Level = 62) are employed to emulate the electrical characteristics of the fabricated micro-LED and TFTs. The simulation of the proposed circuit is carried out by HSPICE simulator based on micro-LED displays with a size of 5.23 inches, a frame rate of 120 Hz, and a resolution of 160 $\times$ 135. The design parameters, including the aspect ratios of TFTs, the capacitances of capacitors, the voltage levels of scan and power lines, and the equivalent model of the micro-LED are listed in Table 1.

Fig. 6(a) shows the simulated waveforms of $V_A$ and $V_C$ with $\pm$ 0.3 V $V_{TH}$ variations of T1 and T2 and $V_{DD}$ I-R drop of 1.2 V. When $\Delta V_{TH}$ is 0 V, 0.3 V, and $-0.3$ V, $V_A$ and $V_C$ both rise to 4.799 V, 5.096 V, and 4.505 V at the end of the CU compensation period since nodes A and C are connected to each other. The differences are 0.297 V and $-0.294$ V, which are close to the $V_{TH}$ variations of T2. In the emission period, $V_C$ remains at the voltages that are stored in C2, and $V_A$ is coupled to $-1.134$ V, $-2.021$ V, and $-2.614$ V by C1. The differences in $V_A$ are $-0.887$ V and $-1.480$ V, including the $V_{TH}$ variations of $\pm$0.3 V and $V_{DD}$ I-R drop of 1.2 V, confirming effective compensation. Moreover, Fig. 6(b) schematically depicts a conventional 2T1C circuit based on p-type TFTs [23], [24], [25]. The 2T1C circuit is the simplest structure adopted in active-matrix micro-LED displays. However, the circuit without any compensation suffers from non-uniform luminance of the displays. Figs. 7(a) and 7(b) compare the proposed circuit with the conventional 2T1C circuit when $V_{TH}$ varies by $\pm$ 0.3 V and $V_{DD}$ drops by 1.2 V. The emission currents that are produced by the proposed circuit are highly uniform and the current error rates are less than 1.65%. In contrast, the 2T1C circuit without compensation exhibits dramatic variations in emission currents. The current error rates of the 2T1C circuit exceed 59.40% at all gray levels and

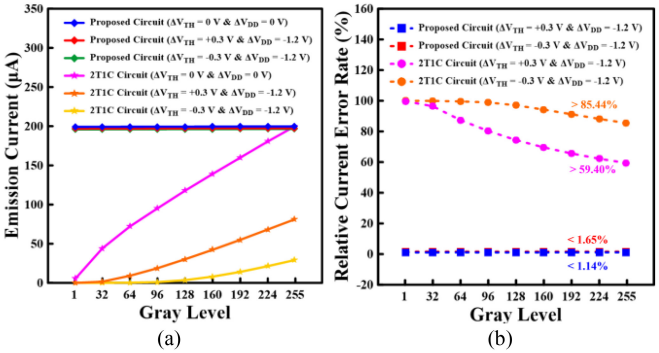


**FIGURE 7.** (a) Emission currents and (b) relative current error rates of proposed circuit compared to 2T1C circuit with $V_{TH}$ variations ($\Delta V_{TH}$ = ±0.3 V) of T1 and T2 and $V_{DD}$ I-R drop ($\Delta V_{DD}$ = −1.2 V) at various gray levels.

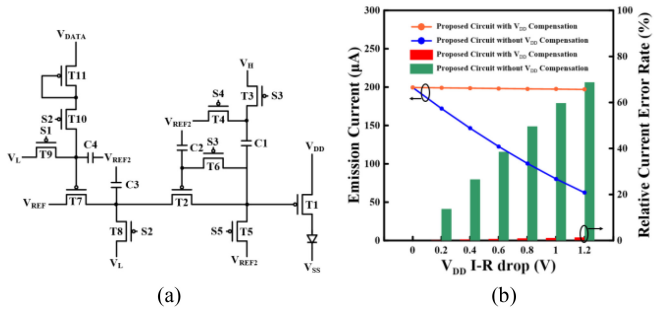


**FIGURE 8.** (a) Schematic of proposed circuit without $V_{DD}$ compensation. (b) Emission currents and relative current error rates of proposed circuit with and without $V_{DD}$ compensation under $V_{DD}$ I-R drops within a range of 1.2 V.

even reach 99.99% at low gray levels, seriously influencing image quality. To further validate the necessity of $V_{DD}$ compensation, an analysis is conducted on the proposed circuit with and without $V_{DD}$ compensation. Fig. 8(a) schematically depicts the proposed circuit without $V_{DD}$ compensation. The gate voltage of T1 cannot be adjusted for various $V_{DD}$ drops, so the $V_{SG}$ of T1 varies. Fig. 8(b) plots the emission currents and the relative current error rates of the proposed circuit with and without $V_{DD}$ compensation under the $V_{DD}$ I-R drops within a range of 1.2 V. The proposed circuit with $V_{DD}$ compensation is immune to $V_{DD}$ I-R drops. However, without $V_{DD}$ compensation, the emission current significantly decreases by 68.80% with a $V_{DD}$ drop of 1.2 V.

In addition, the sweep generation and PWM control of the proposed circuit are investigated in Fig. 9. While generating a sweep waveform, T7 can remain in the saturation region to charge node D from −2.5 V to 7 V with a constant current. The voltage change is linear with time, so the slopes of the voltage waveforms are constant. As $V_{DATA}$ increases, the slope of the sweep waveform decreases. The different pulse widths of emission currents are generated to distinguish gray levels, achieving the analog PWM method. To prevent the impact of the $V_{TH\_T7}$ variations on gray level control, $V_{TH\_T11}$ is stored at node E to compensate for $V_{TH\_T7}$. Fig. 10(a) shows $V_E$ increases to 9.328 V, 9.628 V,

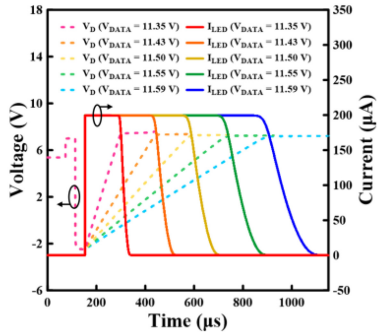


**FIGURE 9.** Transient waveforms of $V_D$ and $I_{LED}$ when different $V_{DATA}$ values are applied.

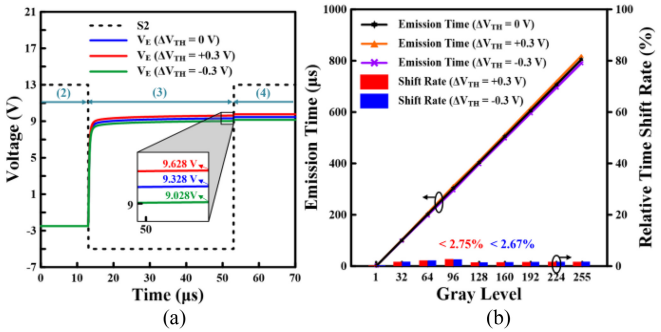


**FIGURE 10.** (a) Transient waveforms of $V_E$ and (b) emission times and relative time shift rates at various gray levels with $V_{TH}$ variations ($\Delta V_{TH}$ = ±0.3 V) of T7 and T11.

and 9.028 V, and the $V_{TH}$ variations of ± 0.300 V are detected during the SG compensation period. The shift rates of emission time with variations in $V_{TH}$ of T7 and T11 by ± 0.3 V at various gray levels are calculated to evaluate the compensation effectiveness. The time shift rates are expressed as the following equation.

$$\text{Time shift rate} = \frac{|T_{VARIED} - T_{UNVARIED}|}{T_{UNVARIED}} \times 100\% \quad (4)$$

where $T_{VARIED}$ and $T_{UNVARIED}$ are the emission times with and without the $V_{TH\_T7}$ and $V_{TH\_T11}$ variations. Fig. 10(b) presents the emission times are almost unchanged and the relative time shift rates are all below 2.75% despite the variations in $V_{TH\_T7}$.

Fig. 11 shows the power comparison of the proposed circuit with that of the 7T1C circuits. The power consumption and its improvement are expressed as the following equations.

$$\text{Power consumption} = I_{LED} \times V_{SUPPLY} \times \text{Emission duty} \quad (5)$$

$$\text{Improvement} = \frac{|P_{PROPOSED} - P_{7T1C}|}{P_{7T1C}} \times 100\% \quad (6)$$

where $V_{SUPPLY}$, $P_{PROPOSED}$, and $P_{7T1C}$ are the difference between $V_{DD}$ and $V_{SS}$, the power consumption of the proposed circuit, and the power consumption of the 7T1C circuit, respectively. Table 2 presents the design parameters of the 7T1C circuit. To make an objective comparison, the

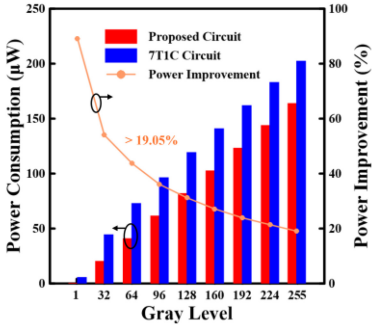


**FIGURE 11.** **Power consumption of proposed circuit and its improvement relative to 7T1C circuit at various gray levels.**

**TABLE 2.** **Design parameters of 7T1C PAM circuit.**

| 7T1C PAM Circuit | | | |
|---|---|---|---|
| **Parameter** | **Value** | **Parameter** | **Value** |
| $(W/L)_{T1, T2, T6}$ (μm/μm) | 162 / (3+3) | $V_{SS}$ (V) | -1.5 |
| $(W/L)_{T3\text{-}T5, T7}$ (μm/μm) | 5 / (3+3) | S1, S2, EM (V) | -5 ~ 13 |
| C1 (pF) | 2 | $V_{DATA}$ (V) | 5.07 ~ 9 |
| $V_{DD}$ (V) | 9 | $V_{INI}$ (V) | -1.5 |

TFTs and C1 of the 7T1C circuit are set the same as those of the proposed circuit to ensure identical driving and voltage stabilization capability. Fig. 11 shows that the power consumption of the proposed circuit is lower than that of the 7T1C circuit at all gray levels. The proposed circuit yields a power improvement of over 19.05% compared to the 7T1C circuit.

## IV. CONCLUSION

A micro-LED pixel circuit with analog PWM based on p-type LTPS TFTs is proposed. The proposed circuit can generate sweep waveforms and emission currents to drive micro-LED. By PWM control, micro-LED operates at high luminous efficiency, lowering the power consumption of the micro-LED displays. Simulation results show that the proposed circuit compensates for the $V_{TH}$ variations of TFTs and $V_{DD}$ I-R drops to provide uniform emission current waveforms. The current error rates are less than 1.65%, and the time shift rates are below 2.75%. In contrast to the 7T1C PAM circuit, the proposed circuit consumes less power and achieves an improvement of at least 19.05%. Consequently, the proposed circuit is prospective for application in micro-LED displays.

## REFERENCES

[1] E.-L. Hsiang, Z. Yang, Q. Yang, P.-C. Lai, C.-L. Lin, and S.-T. Wu, "AR/VR light engines: Perspectives and challenges," *Adv. Opt. Photon.*, vol. 14, pp. 783–861, Nov. 2022.
[2] Q. Chen, D. Geng, Y. Su, X. Duan, H. Ji, and L. Li, "A novel dynamic time method for organic light-emitting diode degradation estimation in display application," *IEEE Electron Device Lett.*, vol. 42, no. 6, pp. 887–890, Jun. 2021.
[3] P.-T. Liu and L.-W. Chu, "Innovative voltage driving pixel circuit using organic thin-film transistor for AMOLEDs," *J. Display Technol.*, vol. 5, no. 6, pp. 224–227, Jun. 2009.
[4] Y.-H. Tai, C.-H. Lin, S. Yeh, C.-C. Tu, and K.-S. Karim, "LTPS active pixel circuit with threshold voltage compensation for X-ray imaging applications," *IEEE Trans. Electron Devices*, vol. 66, no. 10, pp. 4216–4220, Oct. 2019.
[5] S.-P. Huang et al., "Effect of ELA energy density on self-heating stress in low-temperature polycrystalline silicon thin-film transistors," *IEEE Trans. Electron Devices*, vol. 67, no. 8, pp. 3163–3166, Aug. 2020.
[6] C.-L. Lin, C.-C. Hung, P.-Y. Kuo, and M.-H. Cheng, "New LTPS pixel circuit with AC driving method to reduce OLED degradation for 3D AMOLED displays," *J. Display Technol.*, vol. 8, no. 12, pp. 681–683, Dec. 2012.
[7] C.-L. Lin et al., "Compensation pixel circuit to improve image quality for mobile AMOLED displays," *IEEE J. Solid-State Circuits*, vol. 54, no. 2, pp. 489–500, Feb. 2019.
[8] J.-H. Lee et al., "Correlation between the compensation time and the current deviation of organic LED pixel circuit," *J. Soc. Inf. Display*, vol. 28, no. 11, pp. 882–891, Nov. 2020.
[9] W. Guo et al., "The impact of luminous properties of red, green, and blue mini-LEDs on the color gamut," *IEEE Trans. Electron Devices*, vol. 66, no.5, pp. 2263–2268, May 2019.
[10] Y. Huang, E.-L. Hsiang, M.-Y. Deng, and S.-T. Wu, "Mini-LED, micro-LED and OLED displays: Present status and future perspectives," *Light Sci. Appl.*, vol. 9, p. 105, Jun. 2020.
[11] M.-Y. Deng et al., "Reducing power consumption of active-matrix mini-LED backlit LCDs by driving circuit," *IEEE Trans. Electron Devices*, vol. 68, no. 5, pp. 2347–2354, May 2021.
[12] C.-L. Lin et al., "AM PWM driving circuit for mini-LED backlight in liquid crystal displays," *IEEE J. Electron Devices Soc.*, vol. 9, pp. 365–372, 2021.
[13] Y.-H. Hong, E.-K. Jung, S. Hong, and Y.-S. Kim, "61–2: A novel micro-LED pixel circuit using n-type LTPS TFT with pulse width modulation driving," *J. Soc. Inf. Display*, vol. 52, no. 1, pp. 868–871, May 2021.
[14] J. Oh et al., "Pixel circuit with P-type low-temperature polycrystalline silicon thin-film transistor for micro light-emitting diode displays using pulse width modulation," *IEEE Electron Device Lett.*, vol. 42, no. 10, pp. 1496–1499, Oct. 2021.
[15] K.-R. Jen et al., "P-27: A novel PWM driving pixel circuit with metal-oxide TFTs for microLED displays," *J. Soc. Inf. Display*, vol. 53, no. 1, pp. 1137–1140, Jun. 2022.
[16] P.-A. Zou et al., "A new analog PWM pixel circuit with metal oxide TFTs for micro-LED displays," *IEEE Trans. Electron Devices*, vol. 69, no. 8, pp. 4306–4311, Aug. 2022.
[17] C.-L. Lin et al., "AM mini-LED backlight driving circuit using PWM method with power-saving mechanism," *IEEE J. Electron Devices Soc.*, vol. 10, pp. 256–262, 2022.
[18] W.-J. Ma, J.-Y. Yang, H.-Y. Pan, F.-T. Pai, and C.-C. Lin, "P-39: The IR drop compensation method of AMOLED display for dynamic power control," *J. Soc. Inf. Display*, vol. 53, no. 1, pp. 1196–1199, Jun. 2022.
[19] J. Kim, Y.-S. Kim, D. Oh, J. Oh, and T. Shigeta, "Display module," U.S. Patent 11, 551, 605, B2, Jan. 10, 2023.
[20] S.-H. Jung, W.-J. Nam, and M.-K. Han, "A new voltage-modulated AMOLED pixel design compensating for threshold voltage variation in poly-Si TFTs," *IEEE Electron Device Lett.*, vol. 25, no. 10, pp. 690–692, Oct. 2004.
[21] A. Nathan, G.-R. Chaji, and S.-J. Ashtiani, "Driving schemes for a-Si and LTPS AMOLED displays," *J. Display Technol.*, vol. 1, no. 2, pp. 267–277, Dec. 2005.
[22] Y. Kim, Y. Kim, and H. Lee, "A novel p-type LTPS TFT pixel circuit compensating for threshold voltage and mobility variations," *J. Display Technol.*, vol. 10, no. 12, pp. 995–1000, Dec. 2014.
[23] G. Gu and S.-R. Forrest, "Design of flat-panel displays based on organic light-emitting devices," *IEEE J. Sel. Topics Quantum Electron.*, vol. 4, no. 1, pp. 83–99, Jan./Feb. 1998.
[24] M. Stewart, R.-S. Howell, L. Pires, M.-K. Hatalis, W. Howard, and O. Prache, "Polysilicon VGA active matrix OLED displays-technology and performance," in *Proc. IEDM Tech. Dig.*, Dec. 1998, pp. 871–874.
[25] M. Kimura et al., "Low-temperature polysilicon thin-film transistor driving with integrated driver for high-resolution light emitting polymer display," *IEEE Trans. Electron Devices*, vol. 46, no. 12, pp. 2282–2288, Dec. 1999.